Article

Promoting Effect of Inorganic Alkali on Carbon Dioxide Adsorption in Amine-Modified MCM-41

Yang Teng [1], Lijiao Li [1], Gang Xu[1], Kai Zhang [1,*] and Kaixi Li [2]

[1] Beijing Key Laboratory of Emission Surveillance and Control for Thermal Power Generation, North China Electric Power University, Beijing 102206, China; df4d3097@126.com (Y.T.); llj_4324648@126.com (L.L.); xugang6216@163.com (G.X.)

[2] Key Laboratory of Carbon Materials, Institute of Coal Chemistry, Chinese Academy of Sciences, Taiyuan 030001, Shanxi, China; likx@sxicc.ac.cn

* Correspondence: kzhang@ncepu.edu.cn; Tel.: +86-10-6177-2413

Abstract: Three kinds of inorganic alkali are introduced into tetraethylenepentamine (TEPA)- and polyethyleneimine (PEI)-modified MCM-41 as the CO_2 adsorbents. FT-IR and TGA are used to characterize the surface groups and the thermal stability of adsorbents. Chemical titration method is used to measure the alkali amounts of adsorbents. Thermo-gravimetric analysis with 10% CO_2/90% N_2 as the simulated flue gas is used to test the CO_2 adsorption performance of adsorbents. The results show that all three kinds of inorganic alkali-containing adsorbents exhibit higher CO_2 adsorption capability than traditional TEPA and PEI modified samples. $Ca(OH)_2$ and PEI modified samples exhibit the highest adsorption capacity and recyclable property. The introduction of inorganic alkali changes the chemical adsorption mechanism between CO_2 and adsorbent surface due to the increased hydroxyl groups. The CO_2 adsorption capacities have a linear dependence relation with the alkali amounts of adsorbents, indicating that alkali amount is a critical factor for the exploration of novel adsorbents.

Keywords: amine-modified MCM-41; CO_2 adsorption; inorganic alkali; alkali amounts

1. Introduction

The requirement for energy grows rapidly with economic development. In the next few decades, fossil fuels will still be the major energy supply. The proportion of energy currently coming from fossil fuels is around 98% globally. The increase in fossil fuel utilization, correlating with higher CO_2 emissions, has become a serious concern [1]. In addition, continuous uncontrolled CO_2 emissions may contribute to many environmental deteriorations, such as sea level increases and species extinction. For the past few years, CO_2 capture has received significant attention and is being recognized as an urgent mission [2].

The current CO_2 capture technologies mainly include liquid absorption [3], solid adsorption [4–6], membrane purification [7], and cryogenic process [8]. Among these approaches, liquids absorption is widely known and frequently used, but is inevitably accompanied by some disadvantages, such as liquids pollution and equipment corrosion. Solid adsorption could avoid these problems, and demonstrates promising efficiencies.

The key factor for adsorption efficiencies is the adsorbents. A wide variety of materials has been investigated as CO_2 adsorbents, including metal oxides [9], activated carbons [10], zeolites [11,12], and metal-organic frame-works [13]. Alkali metal or alkaline earth metal oxides-based adsorbents have achieved high CO_2 adsorption capacity [14]. However, these materials have slow adsorption kinetics and require high temperature for complete regeneration. Mesoporous silicas modified with basic groups are claimed to be potentially effective materials due to the synergistic effect of physical adsorption and chemical adsorption. Abundant works have focused on this kind of material and have achieved continuous progress. There are two main approaches to the introduction of amine groups to porous materials. One is the impregnation of liquid amine (such as polyethylenimine (PEI) [4] and

tetraethylenepentamine (TEPA) [5]) to disperse amine sites on the support. The other is post-synthesis by grafting aminosilanes to a silica surface. Xu et al. [4,15] dispersed polyethylenmine into the channels of MCM-41 to obtain novel CO_2 adsorbents, and proposed the concept of a "molecular basket". Recent research focused on the latter method, because grafting provides a more stable structure and superior CO_2 adsorption capacities. Chen et al. [6] impregnated PEI on HMS zeolite with three-dimensional pore structure and achieved the highest adsorption capacity of 184 mg/g CO_2 at a PEI loading of 60 wt%. Liu et al. [16] studied the CO_2 performance of triethanolamine-impregnated SBA-15 and found that the adsorption capacity increased by seven times compared with SBA-15 precursor. Yue et al. [5,17] employed DEA and TEPA as the amine source, and calcinated and uncalcinated SBA-15 as the precursor to prepare CO_2 adsorbents. Their results show that increasing amine loading decreased the surface area of SBA-15. Hydroxy groups on uncalcinated SBA-15 has a promoting effect on CO_2 adsorption. Wei et al. [18] impregnated MCM-41 with three kinds of amines, namely diethylenetriamine (DETA), triethylenetetramine (TETA), and 2-amino-2-methyl-1-propanol (AMP), and found that the sample impregnated by TETA showed the highest CO_2 adsorption capacity. Su et al. [19] prepared TEPA-modified commercial Y-type zeolite with and studied their characterizations and adsorption/desorption properties of CO_2. They found that the surface nature of Y zeolite was changed after TEPA modification, which causes a significant enhancement in CO_2 adsorption capacity. Our previous work focused on the effect of amine types to the amine-based MCM-41 materials and found that TEPA and PEI-1800 demonstrated superior CO_2 adsorption capability and stability compared with the others [20]. However, their adsorption capacities need to be further improved by modification.

Numerous works have reported on CO_2 adsorption in amine-based adsorbents, but most works focused on the amine type and the textural structure of materials. The works concerning the effect of inorganic components to amine-based adsorbents are rare. In this work, siliceous MCM-41 is chosen as the substrate. Organic amines and inorganic alkalis are both introduced to MCM-41 to prepare the CO_2 adsorbents. Three kinds of hydroxide are used as inorganic alkali due to their solubility in water during preparation. The purpose of this work is to explore how the organic amines and inorganic alkalis interact with CO_2 molecules. The results are aimed to explain the effective active sites for CO_2 adsorption of adsorbent materials.

2. Experimental

2.1. Materials Preparation

Siliceous MCM-41 was prepared in the presence of cetyltrimethylammonium bromide (CTAB) and tetraethylorthosilicate (TEOS) according to the procedure reported elsewhere as the substrate. The modification of MCM-41 by organic amines was conducted by wet impregnation method. A 40% mass loading of amine to MCM-41 was used, according to our previous results [21]. In a typical procedure, a desired amount of TEPA was dissolved in 10 mL dry ethanol. The mixture is stirred to make the amines dissolved, and then 0.5 g of MCM-41 was added. The obtained slurry was continuously stirred at room temperature until sufficiently blended and was then sealed to stand for 12 h in air, followed by drying for 8 h at 80 °C in a drying oven. The modification of MCM-41 by inorganic alkali was also conducted by impregnation method. Unlike amine modification, the solvent was deionized water and the drying temperature was 100 °C. A 1% mass loading of inorganic alkali to MCM-41 is conducted. The composite modification of organic and inorganic alkali of MCM-41 was conducted following the sequence of inorganic alkali first, and then organic amines.

2.2. Materials Characterization

The crystal structures of all MCM-41 and modified MCM-41 adsorbents were characterized by X-ray diffraction (XRD) on a D8 ADVANCE (Bruker, German) diffractometer operating at 40 kV and 30 mA with CuKα radiation (0.1541 nm). The XRD diffraction patterns were taken in the 2θ range of 1.3°–10° at a scan speed of 0.5°·min^{-1}.

Pore diameter, volume, and surface area of the samples synthesized were evaluated via N_2 physical adsorption analysis through ASAP2020 (Micromeritics, USA) automatic adsorption system. Each sample was degassed at 623 K and 1.33 Pa under N_2 flow for 5 h prior to measurement. The N_2 adsorption data was recorded at the liquid N_2 temperature (77 K). The surface area and the pore size distribution were calculated by the BET and BJH equations, and the total pore volume was estimated from the amount of adsorbed N_2 at the partial pressure $P/P_0 = 0.99$.

Infrared spectra of alkali modified MCM-41s was recorded in the 4000–450 cm^{-1} region using Spectrum 100 FT-IR (PerkinElmer, USA). The alkali quantity of alkali-modified MCM-41s was measured by titration method. In a typical process, 0.5 g samples were added into 25 mL of 0.1 mol/L HCl, then ultrasonically vibrated at room temperature for 24 h and filtered. Ten milliliters of filtrate were added to a conical flask and titrated with NaOH. The alkali quantity was calculated by the NaOH addition.

Thermo-gravimetric analysis (TGA) (TA Q500 US) was applied to determine the thermal stability of adsorbents. From a series of experiments, it was determined to treat the materials at 100 °C for a period of 60 min in N_2 to remove all the water and CO_2 adsorbed from the air. After the initial treatment, a heating rate of 10 °C·min^{-1} up to 800 °C in N_2 was conducted to calculate the real amine impregnated on substrates.

2.3. CO_2 Adsorption

CO_2 adsorption and desorption measurements are also performed on TGA. A gas mixture of 10% CO_2 and 90% N_2 was used as the model flue gas. In each run, about 3 mg of adsorbent sample was loaded into an alumina sample pan, and then pretreated at 100 °C for 1 h in N_2 to remove the adsorbed moisture, followed by cooling to the adsorption temperature of 35 °C prior to its exposure to CO_2. The desorption run was conducted in a pure N_2 flow at 100 °C to achieve complete desorption. In the cycling experiments, five times adsorption and desorption circulation was conducted by repeating the above process. A baseline without samples was conducted at the same condition, and the data in the results has undergone the subtraction.

3. Results and Discussion

3.1. Preparation and Characterization of the Adsorbents

MCM-41s were modified with inorganic alkalis and organic amines. Figure 1 shows the XRD patterns of MCM-41 substrates and modified MCM-41s. For pure MCM-41, a sharp diffraction peak at $2\theta = 1.9°$ is assigned to the 100 face of MCM-41 structure [22]. The XRD patterns of MCM-41-TEPA and MCM-41-PEI also show the characteristic behavior of MCM-41 structure, but the peak intensity of the 100 face was decreased. This is caused by the amines filling the MCM-41 pores. For inorganic alkali-modified materials, the intensity decline is obvious and the decline order is CsOH > KOH > $Ca(OH)_2$. This order is consistent with the alkalinity of hydroxide. This result suggests that the crystal structure of MCM-41 is partly destroyed by strong base solutions during preparation. However, according to the results, the pore structure is not completely destroyed.

Table 1 lists the textural properties of MCM-41 and various modified MCM-41s, as calculated from N_2 adsorption isotherms. The results indicate that the surface area of all the modified MCM-41s decreased compared with pure MCM-41. The decrease of average pore size of modified materials is identical with the surface areas. This can be explained by the pore filling of MCM-41, and the results is in accordance with XRD patterns. The surface area decline of CsOH and KOH modified materials

is also obvious in that of $Ca(OH)_2$ modified materials, which can also be explained by structure collapse.

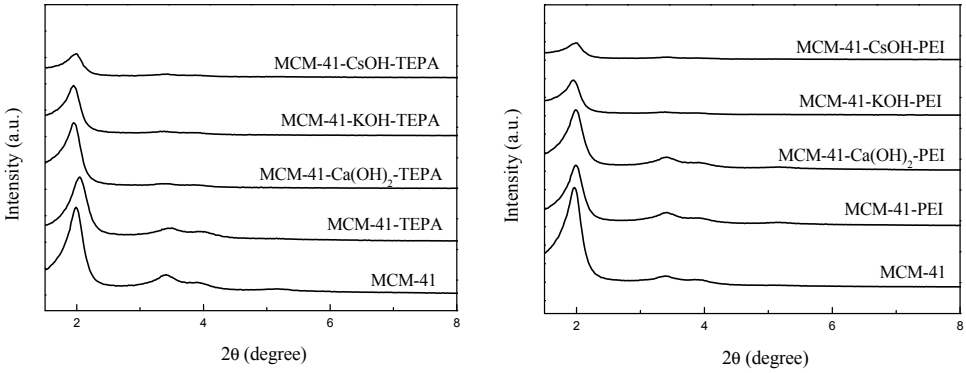

(**a**) (**b**)

Figure 1. XRD patterns of MCM-41 modified by (**a**) tetraethylenepentamine (TEPA) (**b**) polyethylenimine (PEI) and various alkali components.

Table 1. Pore structure parameters of various adsorbents.

Materials	Surface Areas (m^2/g)	Pore Volume (cm^3/g)	Average Pore Diameters (nm)
MCM-41	865	1.00	4.64
MCM-41-TEPA	431	0.83	2.21
MCM-41-KOH-TEPA	322	0.97	2.15
MCM-41-$Ca(OH)_2$-TEPA	405	0.94	2.31
MCM-41-CsOH-TEPA	293	0.97	2.61
MCM-41-PEI	508	0.98	2.54
MCM-41-KOH-PEI	391	1.08	2.33
MCM-41-$Ca(OH)_2$-PEI	411	1.12	2.50
MCM-41-CsOH-PEI	306	0.91	2.14

The surface functional groups of adsorbent samples are confirmed by FT-IR spectra. Figure 2a shows the spectra of samples containing TEPA as the organic amine. The bands at 800 cm^{-1} and 1084 cm^{-1} are attributed to the ν_{as}(Si-O-Si) and ν_s(Si-O-Si) of MCM-41 [23]. The bands at 1475 cm^{-1}, 1570 cm^{-1}, and 1650 cm^{-1} represent the δ_s(C-H), δ_{as}(N-H), and δ_s(O-H), indicating the presence of $–NH_2$ in samples [24]. Additionally, the band at 3430 cm^{-1} is characteristic of the (Si-)OH stretch. Comparing the spectrum of inorganic-containing MCM-41-TEPA samples with MCM-41-TEPA, the bands at 1475 cm^{-1}, 1570 cm^{-1}, and 1650 cm^{-1} all increase, which indicate that the presence of inorganic alkali enhance the infrared activity of amine groups. After the inorganic alkali impregnation, the MCM-41 surface is seriously changed. Therefore, the distribution of organic amine molecules in the outer surface should be increased. The FT-IR spectra in Figure 2b correspond to PEI and different inorganic alkali modified samples. Surprisingly, PEI modified samples behave similarly in terms of FT-IR properties to the TEPA modified samples, in that inorganic alkali-containing samples exhibit obvious FT-IR bands corresponding to $-NH_2$ characteristics.

Preprints (www.preprints.org) | NOT PEER-REVIEWED | Posted: 22 August 2016 doi:10.20944/preprints201608.0189.v1

Peer-reviewed version available at Energies 2016, 9, 667; doi:10.3390/en9090667

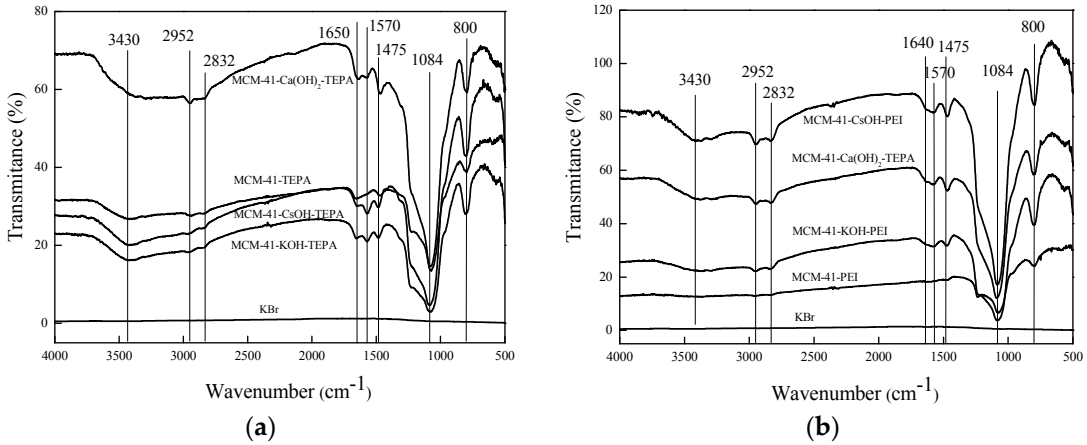

Figure 2. FT-IR spectra of MCM-41 modified by (**a**) TEPA (**b**) PEI and various alkali components.

The thermal stability of amines and various inorganic alkali-modified MCM-41s was evaluated by TGA, and the curves are shown in Figure 3a,b. For TEPA-modified samples (as shown in Figure 3a), there are two main obvious weight loss processes in the curves. The first stage is from room temperature to 120 °C with a mass loss of around 3%, which is attributed to the moisture evolving, and the second stage from 120 °C to 400 °C with a loss of around 30% is due to the degradation of amines. The actual amine loadings can be determined by the weight loss of the second stage. The weight losses of four samples at this stage are comparable to each other at around 30%, which is lower than the calculated value of 40% added at impregnation. This may be caused by the amine volatilization during the drying process. The weight loss difference of four samples may be due to the tiny difference of combination force between amine and MCM-41 influenced by inorganic alkali species. The TGA curves of PEI modified samples in Figure 3b show that the initial decomposition temperature of PEI is above 200 °C, which is higher than TEPA. This indicates that PEI-modified adsorbents possess better thermal stabilities and can be applied for long-term use at relatively high temperatures compared to TEPA. Contrasting the curves of TEPA-modified samples in Figure 2a, the weight loss takes place in a narrower temperature range. The faster weight loss rate of PEI-modified samples confirms that PEI degrades more quickly than TEPA at temperature-programmed conditions. The importance of alkali loadings to CO_2 adsorption capacities has been confirmed by researchers [25]. From the TGA curves, it is obvious that similar weight loadings are achieved for all eight samples with various alkali species. However, as will be shown further in the text, the effective alkali amounts for CO_2 adsorption are different from each other.

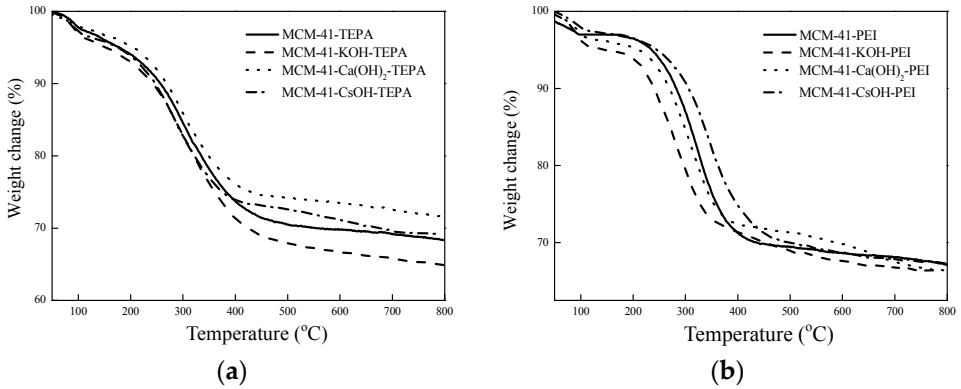

Figure 3. TGA curves of MCM-41 modified by (**a**) TEPA (**b**) PEI and various alkali components.

The adsorbent materials were dissolved in HCl, and the solution was titrated by NaOH to give the effective alkali amounts. Table 2 gives the average values of three repeated experiments. The data shows that both MCM-41-TEPA and MCM-41-PEI have the lowest alkali amounts compared with

inorganic alkali-containing materials, and $Ca(OH)_2$ modified samples have the highest values. From the chemical composition of these three alkali components, $Ca(OH)_2$ posses two hydroxyls, and the other two alkali have only one. This may be why the highest alkali amounts were obtained on $Ca(OH)_2$-containing materials. As it is known that chemical adsorption plays an important role during CO_2 adsorption on alkali-modified adsorbents, the surface basicity should be the key parameter [26]. The alkali amounts reflect the surface basicity of adsorbents and further on the effective active sites for chemical adsorption with CO_2.

Table 2. Alkali amounts of various adsorbents.

Materials	NaOH solution ($\overline{V}$ /mL)	Alkali Amounts/(mmol/g)
MCM-41-TEPA	11.81	0.8812
MCM-41-KOH-TEPA	8.91	1.1607
MCM-41-$Ca(OH)_2$-TEPA	4.35	1.6001
MCM-41-CsOH-TEPA	8.82	1.1693
MCM-41-PEI	12.48	0.7819
MCM-41-KOH-PEI	6.73	1.3708
MCM-41-$Ca(OH)_2$-PEI	5.86	1.4546
MCM-41-CsOH-PEI	6.35	1.4074

3.2. CO_2 Adsorption Performance of Adsorbents

Figure 4 shows the adsorption curves of MCM-41-TEPA and MCM-41-PEI in 10% CO_2/90% N_2 measured by TGA. The samples were first dried by heating to 110 °C and were then cooled to 50 °C in pure N_2. It can be seen that MCM-41-TEPA and MCM-41-PEI have comparable adsorption performance. The adsorption rate of MCM-41-TEPA is slightly faster than that of MCM-41-PEI, and the adsorption capacity of MCM-41-TEPA is higher. The calculated saturation capacities are 0.512 mmol/g for MCM-41-TEPA and 0.663 mmol/g for MCM-41-PEI. As the pure MCM-41 has poor adsorption capacity [15], most of the adsorption capability contribution is from the amines impregnation.

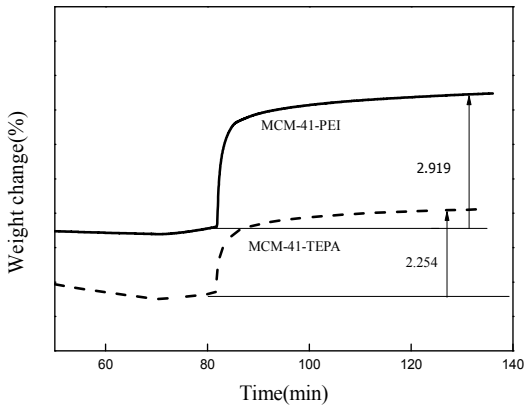

Figure 4. CO_2 adsorption curves of MCM-41-TEPA and MCM-41-PEI.

Following the same procedure as the curves above, the adsorption curves of various inorganic containing adsorbents are given in Figure 5a,b. Figure 4a shows the adsorption curves of MCM-41-TEPA and inorganic alkali-modified MCM-41-TEPAs. It can be seen that for MCM-41-TEPA-KOH and MCM-41-TEPA-CsOH, the adsorption rates are comparable to MCM-41-TEPA, but the adsorption capacities increase. For MCM-41-TEPA-$Ca(OH)_2$, the time to saturate adsorption is obviously shortened, thus showing a faster adsorption rate. The saturation adsorption capacities of all inorganic alkali-modified samples outperform MCM-41-TEPA in the order MCM-41-$Ca(OH)_2$-TEPA > MCM-41-CsOH-TEPA > MCM-41-KOH-TEPA > MCM-41-TEPA. Figure 4b shows that the adsorption performance of inorganic alkali-modified MCM-41-PEIs behave slightly differently from MCM-41-TEPAs. All inorganic alkali-modified samples follow a similar adsorption pattern to that of MCM-41-TEPA, indicating that the adsorption rates are comparable. However, MCM-41-$Ca(OH)_2$-

Peer-reviewed version available at Energies 2016, 9, 667; doi:10.3390/en9090667

PEI shows the highest adsorption capacity among PEI-modified samples. Despite the weak alkali of $Ca(OH)_2$, it behaves superiorly, promoting CO_2 adsorption on amine-modified MCM-41s.

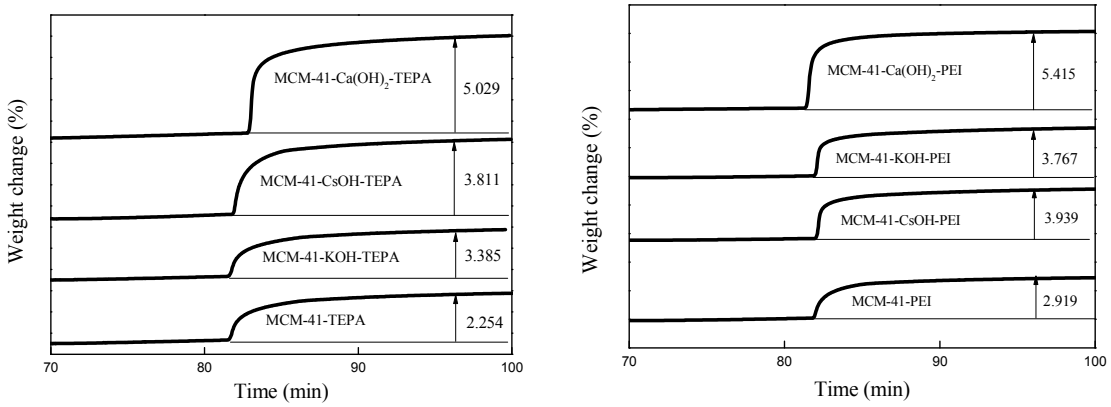

Figure 5. CO_2 adsorption curves of (**a**) TEPA (**b**) PEI and various inorganic alkali-modified adsorbents.

To further understand the CO_2 adsorption and regeneration properties of adsorbent samples, the in situ desorption experiment was conducted in N_2 at 100 °C. Five repeated adsorption/desorption cycles were tested for all samples at the same conditions. Figure 6a shows the cycle performance of TEPA-modified samples. For MCM-41-TEPA, the weight of adsorption after one adsorption/desorption cycle slightly decreases, but the weight gains after each adsorption have no obvious decrease. This may due to that the N_2 flow removes some of TEPA molecules existing on the outer surface of MCM-41. However, the effective adsorption sites on MCM-41-TEPA are not reduced. For MCM-41-KOH-TEPA and MCM-41-CsOH-TEPA, a slight drop in adsorption capacity of 4.8% and 6.9%, respectively, was observed after each cycle. This is because the combinations of KOH or CsOH to CO_2 molecules are irreversible. For MCM-41-$Ca(OH)_2$-TEPA, there is no saturation capacity decrease, which suggests that calcium-based materials have reversible combination to CO_2. In addition, MCM-41-$Ca(OH)_2$-TEPA behaves stable at operated conditions due to its better chemical stability.

Figure 6b shows the cycle adsorption/desorption curves of MCM-41-PEI and inorganic alkali-modified MCM-41-PEI. The curves indicate that the cycle of all PEI modified samples are very stable for both the adsorbents' weight due to the better thermal stability of PEI. However, there is a slight drop in the adsorption capacity for all PEI-modified samples during five runs. The maximum adsorption capacity drop is less than 0.2% which suggests that PEI modified samples have superior regeneration capabilities to TEPA.

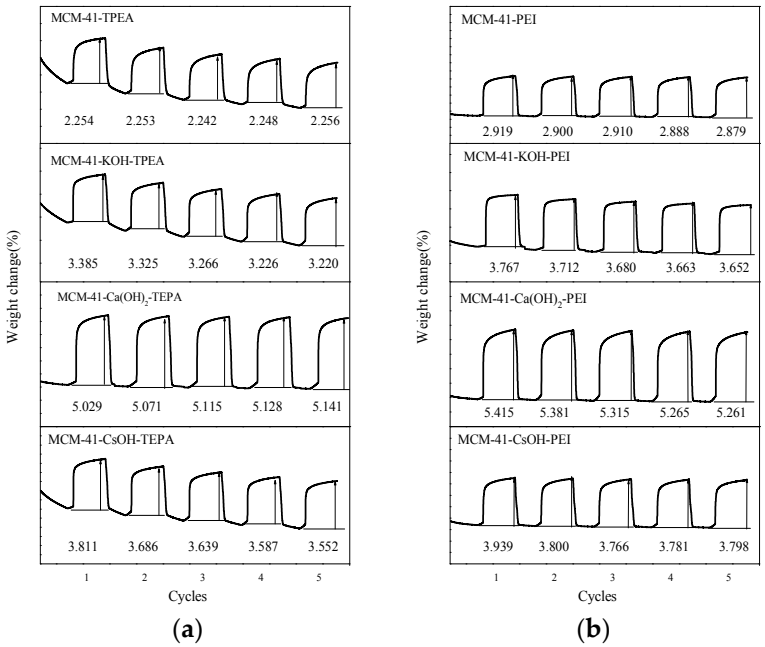

Figure 6. Cycle adsorption/desorption performance of (**a**) TEPA (**b**) PEI and various inorganic alkali modified adsorbents.

3.3. Promoting Effect of Inorganic Alkali

As all the inorganic alkali-containing adsorbents showed superior CO_2 adsorption capacities to the amine modified alone, it is obvious that inorganic alkali plays a promoting effect on the CO_2 adsorption performance of amine-modified MCM-41s. Since chemical adsorption dominates the CO_2 adsorption on amine-modified materials, the chemical reaction should be discussed. Because all the adsorption experiments were conducted at dry conditions, Equations (1) and (2) are believed to be the main reactions:

$$CO_2 + 2RNH_2 \longrightarrow RNCOO^- + RNH_3^+ \quad (1)$$

$$CO_2 + 2R_2NH \longrightarrow R_2NCOO^- + R_2NH_2^+ \quad (2)$$

There is only NH group existing on PEI and NH and NH_2 groups co-exist on TEPA. For inorganic alkali containing adsorbents, there are hydroxyl groups existing. Thus the adsorption reaction should be Equations (3) and (4) [27]:

$$CO_2 + ROH + RNH_2 \longrightarrow RNHCOO^- + ROH_2^+ \quad (3)$$

$$CO_2 + ROH + R_2NH \longrightarrow R_2NCOO^- + ROH_2^+ \quad (4)$$

ROH participates in the reaction and the active sites from the amine are increased by half. If the adsorption on amine and inorganic alkali-modified samples occurs completely in accordance with Equations (3) and (4) and the hydroxyl groups are enough, the saturated capacity should be increased by 2 times. The altering in chemical reaction mechanism should be one reason for the promoting effect.

In order to clarify whether the promoted adsorption capacity is from the inorganic alkali and organic amine, respectively, the adsorption/desorption performance of inorganic alkali alone modified samples were also conducted. The results in Figure 7 indicate that all inorganic alkali-modified samples have very low adsorption capacities. For example, in the case of MCM-41-$Ca(OH)_2$-TEPA, its saturated adsorption capacity is much greater than the sum capacity of MCM-41-TEPA and

Preprints (www.preprints.org) | NOT PEER-REVIEWED | Posted: 22 August 2016 doi:10.20944/preprints201608.0189.v1

Peer-reviewed version available at Energies 2016, 9, 667; doi:10.3390/en9090667

MCM-41-Ca(OH)$_2$. Thus, the reason should be that the existence of inorganic alkali increases the effective alkali amounts of adsorbent materials.

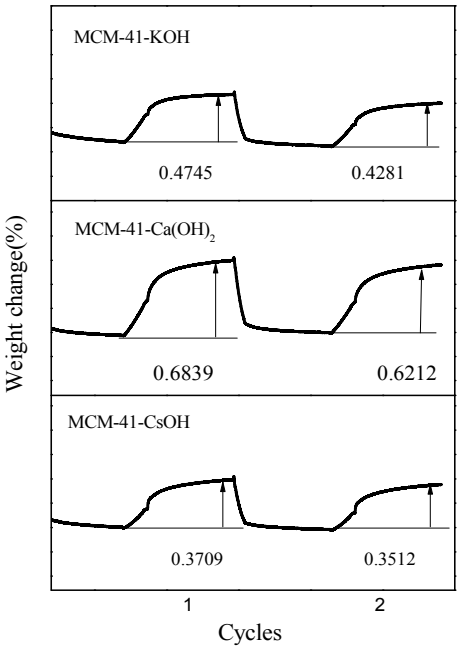

Figure 7. Cycle adsorption/desorption performance of inorganic alkali modified adsorbents.

Figure 8 shows the relationship between the saturation CO_2 adsorption capacities of materials and the effective alkali amounts. It should be noted that the adsorption capacity increased with increasing alkali amounts. This indicates that the effective alkali amount is an important factor for CO_2 adsorption. For Ca(OH)$_2$ and amine co-modified adsorbents, the effective alkali amount is the highest which has the highest adsorption capacity. Compared with three kinds of inorganic alkali, Ca(OH)$_2$ possess the most hydroxyl groups, which should be one reason for the most obvious promoting effect. These results support the results by Yue et al. [17] showing that the hydroxyl groups in the template increased the CO_2 adsorption capacity of amine-containing SBA-15. During the composite modification of organic and inorganic alkali, the surface of MCM-41 undergoes complex changes. Although the framework of MCM-41 partially collapses in alkali solution, the surface OH group increases more or less modified by different alkalis. Thus, the increase of effective OH groups at the material's surface should be a key factor in the future CO_2 adsorbents development.

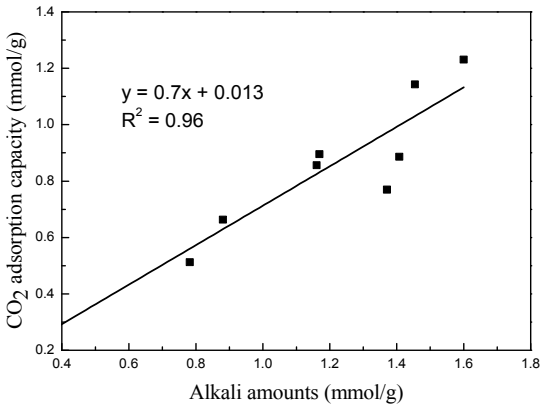

Figure 8. Relationship between CO_2 adsorption capacity and effective alkali amounts.

4. Conclusions

In this study, we have introduced KOH, CsOH, and $Ca(OH)_2$ into TEPA- and PEI-modified MCM-41 as the CO_2 adsorbents. The CO_2 adsorption capabilities of all three kinds of inorganic alkali-containing adsorbents are enhanced compared to TEPA- and PEI-modified samples. Among three kinds of inorganic alkali, $Ca(OH)_2$- and PEI-modified samples exhibit the highest adsorption capacity and stable regeneration property. Hydroxyl groups and adsorbent alkalinity play an important role during CO_2 adsorption. The CO_2 adsorption capacities have a linear dependence with the alkali amounts of adsorbents.

Acknowledgments: Authors gratefully acknowledge National Basic Research Program of China (2015CB251504), National Natural Science Foundation of China (91434120), and Shanxi Province Coal-based Key Scientific and Technological Project (MD2014-09, MD2014-03).

Author Contributions: Yang Teng designed the experiments, analyzed the date and wrote the paper; Lijiao Li performed the experiments; Kai Zhang and Gang Xu analyzed the data and provided the helpful discussion; Kaixi Li contributed analysis tools and provided the helpful discussion.

Conflicts of Interest: The authors declare no conflict of interest.

Abbreviations

The following abbreviations are used in this manuscript:

TEPA	Tetraethylenepentamine
PEI	Polyethyleneimine
CTAB	Cetyltrimethylammonium Bromide
TEOS	Tetraethylorthosilicate
DTEA	Diethylenetriamine
TETA	Triethylenetetramine
AMP	2-amino-2-methyl-1-propanol
TGA	Thermo-gravimetric Analysis

References

1. Gibbins, J.; Chalmers, H. Carbon capture and storage. *Energy Policy* **2008**, *36*, 4317–4322.
2. Schrag, D.P. Preparing to capture carbon. *Science* **2007**, *315*, 812–813.
3. Koronaki, I.P.; Prentza, L.; Papaefthimiou, V. Modeling of CO_2 capture via chemical absorption processes—An extensive literature review. *Renew. Sustain. Energy Rev.* **2015**, *50*, 547–566.
4. Xu, X.; Song, C.; Andersen, J.M.; Miller, B.G.; Scaroni, A.W. Preparation and characterization of novel CO_2 "molecular basket" adsorbents based on polymer-modified mesoporous molecular sieve MCM-41. *Microporous Mesoporous Mater.* **2003**, *62*, 29–45.
5. Yue, M.B.; Chun, Y.; Cao, Y.; Dong, X.; Zhu, J.H. CO_2 capture by as-prepared SBA-15 with an occluded organic template. *Adv. Funct. Mater.* **2006**, *16*, 1717–1722.
6. Chen, C.; Son, W.J.; You, K.S.; Ahn, J.W.; Ahn, W.S. Carbon dioxide capture using amine-impregnated HMS having textural mesoporosity. *Chem. Eng. J.* **2010**, *161*, 46–52.
7. Brunetti, A.; Scura, F.; Barbieri, G.; Drioli, E. Membrane technologies for CO_2 separation. *J. Membr. Sci.* **2010**, *359*, 115–125.
8. Xu, G.; Li, L.; Yang, Y.; Tian, L.; Liu, T.; Zhang, K. A novel CO_2 cryogenic liquefaction and separation system. *Energy* **2012**, *42*, 522–529.
9. Auta, M.; Amat Darbis, N.D.; Mohd, A.T.; Hameed, B.H. Fixed-bed column adsorption of carbon dioxide by sodium hydroxide modified activated alumina. *Chem. Eng. J.* **2013**, *233*, 80–87.
10. Hao, G.P.; Li, W.C.; Lu, A.H. Novel porous solids for carbon dioxide capture. *J. Mater. Chem.* **2011**, *21*, 6447–6451.
11. Siriwardane, R.N.; Shen, M.S.; Fisher, E.P. Adsorption of CO_2, N_2, and O_2 on natural zeolites. *Energy Fuels* **2003**, *17*, 571–576.
12. Bezerra, D.P.; Oliveira, R.S.; Vieira, R.S.; Cavalcante, C.L.; Azevedo, D.C.S. Adsorption of CO_2 on nitrogen-enriched activated carbon and zeolite 13X. *Adsorption* **2011**, 17, 235–246.

13. Herm, Z.R.; Swisher, J.A.; Smit, B.; Krishna, R.; Long, J.R. Metal-organic frameworks as adsorbents for hydrogen purification and precombustion carbon dioxide capture. *J. Am. Chem. Soc.* **2011**, *133*, 5664–5667.
14. Zhao, C.; Chen, X.; Anthony, E.J.; Jiang, X.; Duan, L.; Wu, Y.; Dong, W.; Zhao, C. Capturing CO_2 in flue gas from fossil fuel-fired power plants using dry regenerable alkali metal-based sorbent. *Prog. Energ. Combust.* **2013**, *39*, 515–534.
15. Xu, X.; Song, C.; Andersen, J.M.; Mille, B.G.; Scaroni, A.W. Novel polyethylenimine-modified mesoporous molecular sieve of MCM-41 type as high-capacity adsorbent for CO_2 capture. *Energy Fuels* **2002**, *16*, 1463–1469.
16. Liu, X.; Zhou, L.; Fu, X.; Sun, Y.; Su, W.; Zhou, Y. Adsorption and regeneration study of the mesoporous adsorbent SBA-15 adapted to the capture/separation of CO_2 and CH_4. *Chem. Eng. Sci.* **2007**, *62*, 1101–1110.
17. Yue, M.B.; Sun, L.B.; Cao, Y.; Wang, Z.J.; Wang, Y.; Yu, Q.; Zhu, J.H. Promoting the CO_2 adsorption in the amine-containing SBA-15 by hydroxyl group. *Microporous Mesoporous Mater.* **2008**, *114*, 74–81.
18. Wei, J.; Liao, L.; Xiao, Y.; Zhang, P.; Shi, Y. Capture of carbon dioxide by amine-impregnated as-synthesized MCM-41. *J. Environ. Sci.* **2010**, *22*, 1558–1563.
19. Su, F.; Lu, C.; Kuo, S.C.; Zeng, W. Adsorption of CO_2 on amine-functionalized Y-type zeolites. *Energy Fuels* **2010**, *24*, 1441–1448.
20. Liu, Z.; Teng, Y.; Zhang, K.; Cao, Y.; Pan, W. CO_2 adsorption properties and thermal stability of different amine-impregnated MCM-41 materials. *J. Fuel. Chem. Technol.* **2013**, *41*, 469–475.
21. Liu, Z.; Teng, Y.; Zhang, K.; Chen, H.; Yang, Y. CO_2 adsorption performance of different amine-based siliceous MCM-41 materials. *J. Energy Chem.* **2015**, *24*, 322–330.
22. Kamarudin, K.N.; Alias, N. Adsorption performance of MCM-41 impregnated with amine for CO_2 removal. *Fuel Process. Technol.* **2013**, *106*, 332–337.
23. Liu, L.; Li, H.; Zhang, Y. A comparative study on catalytic performances of chromium incorporated and supported mesoporous MSU-x catalysts for the oxide hydrogenation of ethane to ethylene with carbon dioxide. *Catal. Today* **2006**, *115*, 235–241.
24. Khatri, R.A.; Chuang, S.S.C.; Soong, Y.; Gray, M. Carbon dioxide capture by diamine-grafted SBA-15: A combined fourier transform infrared and mass spectrometry study. *Ind. Eng. Chem. Res.* **2005**, *44*, 3702–3708.
25. Serna-Guerrero, R.; Da'na, E.; Sayari, A. New insights into the interactions of CO_2 with amine-functionalized silica. *Ind. Eng. Chem. Res.* **2008**, *47*, 9406–9412.
26. Zelenak, V.; Halamova, D.; Gaberova, L.; Bloch, E.; Llewellyn, P. Amine-modified SBA-12 mesoporous silica for carbon dioxide capture: Effect of amine basicity on sorption properties. *Microporous Mesoporous Mater.* **2008**, *116*, 358–364.
27. Leal, O.; Bolívar, C.; Ovalles, C.; García, J.J.; Espidel, Y. Reversible adsorption of carbon dioxide on amine surface-bonded silica gel. *Igorg. Chim. Acta* **1995**, *240*, 183–189.